THE ASTROPHYSICAL JOURNAL, 543:328–339, 2000 November 1

PLANETESIMAL ACCRETION IN BINARY STAR SYSTEMS

F. MARZARI
Dipartimento di Fisica, University of Padova, Via Marzolo 8, Padova, Italy 35131; marzari@pd.infn.it
AND
H. SCHOLL
Observatoire de la Cote d'Azur, B.P. 4229, Nice Cedex 4, France F-06304; scholl@obs-nice.fr
Received 2000 March 2; accepted 2000 June 5

ABSTRACT

Planetesimal accretion in close binary systems is a complex process for the gravitational perturbations of the companion star on the planetesimal orbits. These perturbations excite high eccentricities that can halt the accumulation process of planetesimals into planets also in those regions around the star where stable planetary orbits would eventually be possible. However, the evolution of a planetesimal swarm is also affected by collisions and gas drag. In particular, gas drag combined with the secular perturbations of the secondary star forces a strong alignment of all the planetesimal periastra. Since periastra are also coupled to eccentricities via the secular perturbations of the companion, the orbits of the planetesimals, besides all being aligned, also have very close values of eccentricity. This orbital "phasing" strongly reduces the contribution of the eccentricity to the relative velocities between planetesimals, and the impact speeds are dominated by the Keplerian shear: accretion becomes possible. This behavior is not limited to small planetesimals but also affects bodies as large as 100 km in diameter. The effects of gas drag are in fact enhanced by the presence of the constant forced component in the orbital eccentricity of the planetesimals. We describe analytically the periastron alignment by using the secular equations developed by Heppenheimer, and we test the prediction of the theory with a numerical code that integrates the orbits of a swarm of planetesimals perturbed by gas drag and collisions. The gas density is assumed to decrease outward, and the collisions are modeled as inelastic. Our computations are focused on the α Centauri system, which is a good candidate for terrestrial planets as we will show. The impact velocities between planetesimals of different sizes are computed at progressively increasing distances from the primary star and are compared with estimates for the maximum velocity for accretion. According to our simulations in the α Centauri system, the formation of a planet within 2 AU of the primary star is possible because of the orbital phasing forced by gas drag.

Subject headings: binaries: close — celestial mechanics, stellar dynamics — planetary systems — planets and satellites: general — solar system: formation — stars: formation
On-line materials: color figures

1. INTRODUCTION

The formation of planets by accretion around a star is a complex process believed to occur mainly through the following steps: (1) a rotating protostellar disk of gas and dust forms around the star; (2) the dust in the disk accumulates into planetesimals by nongravitational sticking processes; (3) planetesimals collide and gravitationally accrete into larger bodies; and (4) terrestrial planets and cores of giant planets are formed.

Accretion disks have been detected around most T Tauri stars, and recently they have also been directly observed with the *Hubble Space Telescope* (McCaughrean & O'dell 1996). The presence of these disks has been interpreted as evidence of the first step toward the formation of planetary systems similar to our own. The detection of numerous extrasolar planets and the coexistence around the same star of an extrasolar planet and a circumstellar disk (Dominik et al. 1998; Trilling & Brown 1998; Trilling, Brown, & Rivkin 2000) strongly suggest that indeed these disks evolve frequently into planetary systems.

Until recently, it was believed that only single solar-type stars might harbor planetary systems. However, since 1997 three multiple systems with planets have been detected: 16 Cyg B, 55 ρ Cnc, and τ Boo. This important circumstance confirms that planetary formation is not limited to single stars but can also occur in the more frequent multiple-star systems. That the accretion process occurs in a similar way in single and in binary stars is strongly supported by the presence of circumstellar disks around binaries. Observational evidences such as near-infrared excess emission, spectral veiling, Balmer and forbidden emission lines, and polarization (see Mathieu 1994; Mathieu et al. 2000) indirectly suggest the existence of disk material around each individual component of the binary system (circumstellar disk) or around the entire binary star system (circumbinary disk). Direct observations of circumstellar disks have been obtained by Akeson, Koerner, & Jensen (1998) who imaged at high resolution a young binary T Tauri star and detected a small disk around one of the stars smaller than the separation between the two binary components. Rodriguez et al. (1998) imaged two clearly separated circumstellar disks associated with the two components of a binary system in L1551. Their observations suggest circumstellar disks extending for about 10 AU from the star and with masses of 0.06 and 0.03 $M_\odot$, respectively. In spite of the fact that circumstellar disks are tidally truncated at 0.2–0.5 times the binary separation, as also confirmed by the reduction in the millimeter flux of dust emission, it is expected that in general they still have masses comparable to the minimum solar mass model for the solar system (0.01–0.03 $M_\odot$). This

implies that planetary formation in binary systems may be common and may proceed as in our solar system: formation of planetesimals and final accretion of these planetesimals into planets.

One should make a distinction between accretion around a single star and accretion in a binary system. In binary systems the gravitational perturbations of the companion star can interfere, and they may inhibit the planetesimal accumulation process around the other star. While 16 Cyg B and 55 ρ Cnc are rather loose systems, where the distance between the two components is more than 1000 AU, most of the binary systems have separations between 10 and 100 AU. In these cases, the companion may have played an important role either by preventing the formation of planets by increasing the relative velocities among planetesimals or by destabilizing the possible planetary system.

Holman & Wiegert (1999) have investigated the stability of planetary orbits in eccentric binary systems and determined regions of the phase space where planets can persist for long timescales. We study within these stability regions whether or not planetesimal accretion can lead to the formation of planets. There are competing mechanisms that inhibit or favor the formation of planets from a swarm of planetesimals. On the one hand, the strong gravitational perturbations of the companion can increase the relative velocities among planetesimals and collisions might result in disruption rather than accretion. For instance, Whitmire et al. (1998), using a model without collisions and drag forces, found relative velocities among planetesimals inhibiting accretion in many cases also in the stability zones of Holman & Wiegert. On the other hand, several dissipative mechanisms, which include gas drag, viscous stirring, and dynamical friction, can counterbalance the gravitational effects of the secondary star and allow planetesimal accumulation. We will show that gas drag, in particular, plays an important role in reducing the impact velocities. It does not only damp the planetesimals' eccentricities, but it also forces a strong alignment of the planetesimals' periastra. This alignment significantly reduces the impact velocities, favoring the accretion process.

To investigate the planetesimal accretion process, we adopt in this paper a numerical model that includes both the gas drag force and inelastic collisions. The advantage of including collisions is that we can roughly simulate their eventual damping effects on the relative velocities and we can also derive the statistical distribution of the impact velocities. This distribution depends on the planetesimals' orbital elements, which are significantly influenced by the combination of the gravitational perturbation of the companion star and by the dissipative processes. Great relevance resides in the combination of the forced secular perturbations by the companion and the gas drag that leads, as mentioned above, to a strong alignment of the planetesimals' periastra. This phenomenon, already studied by Marzari et al. (1997) for planetesimals in a solar nebula where a proto-Jupiter formed on a short timescale, induces a decrease of the relative velocities as compared with a swarm with no alignment. This is particularly relevant for the accretion process of small planetesimals, where impact velocities of few hundred meters per second can lead to disruption instead of accumulation.

We applied our model to the α Centauri system. For a long time, this system has been suspected to harbor a planetary system, and it also presents a good test case for planetary accretion in the terrestrial region. The separation between the stars is about 24 AU, and the accretion process below 2 AU around the primary star must be put under scrutiny because of the closeness of the companion star. The critical semimajor axis within which stable planetary orbits are possible is within $\sim$2.7 AU from the primary star. However, planetary accretion inside the critical semimajor axis might have been halted by the high eccentricity of the orbits. We assume in our computations that the circumstellar disk is coplanar with the binary orbital plane. This assumption is natural in cloud collapse models; however, little is still known from an observational point of view about the alignment of the circumstellar disks and the binary orbital plane. We assume here that coplanarity is the most probable geometrical configuration.

In § 2 we describe in detail the numerical model we employed in our computations of dynamical and collisional planetesimal evolution. In § 3 we interpret analytically the periastron alignment of planetesimal orbits and we present numerical results confirming the analytical predictions. In § 4 we show that collisions do not significantly alter the alignment even under the hypothesis of a dense planetesimal disk and, then, of a high collision rate. Finally, in § 4.3 we give the distribution of the impact velocities showing how they are significantly damped by the periastron alignment: accretion is favored rather than fragmentation. Section 5 is devoted to a discussion of the results and conclusions.

2. THE NUMERICAL MODEL

In our model, the star α Centauri B moves on a fixed elliptical orbit around the primary component A with a semimajor axis of 23.4 AU and an eccentricity of 0.52. The masses of components A and B are, respectively, 1.1 and 0.9 $M_\odot$. The planetesimals move solely around component A on planar orbits. Besides the gravitational forces exerted by the binaries, the planetesimals may be subjected to gas drag forces. In this case, we assume a gas disk around the primary A, coplanar with the planetesimal disk. In addition, inelastic collisions between planetesimals can be taken into account. Gravitational interactions among the planetesimals are not considered.

The main purpose of our model is to investigate the effects of gas drag and collisions on the velocity distribution of planetesimals. Both effects can be studied separately or combined.

2.1. *Gas Drag*

A gas disk around a star exerts a drag force on the motion of a small body orbiting around the star. The reason is that, because of gas pressure, the velocity of the gas at a given distance from the star is not equal to the Kepler velocity of a body revolving the star at the same distance (Adachi, Hayashi, & Nakazawa 1976). Hence, a planetesimal revolving around α Centauri A and embedded in a gas disk is accelerated because of the gravitational forces of the binaries and, in addition, because of the gas drag force. The latter acceleration can be modeled by (e.g., Marzari et al. 1997)

$$\ddot{\boldsymbol{r}} = -Kv_{\rm rel}\boldsymbol{v}_{\rm rel}\,, \tag{1}$$

where $\boldsymbol{v}_{\rm rel}$ is the velocity of the planetesimal relative to the gas and $v_{\rm rel}$ its modulus.

The drag parameter K (Kary, Lissauer, & Greenzweig 1993) is given by

$$K = \frac{3\rho_g C_d}{8\rho_{\rm pl} s}, \quad (2)$$

with s the radius of the planetesimal, $\rho_{\rm pl}$ its mass density, ρ_g the gas density of the nebula, and C_d a dimensionless drag coefficient ($\simeq 0.4$ for spherical bodies). K is turned into a nondimensional numerical quantity when multiplied by 1 AU.

We assumed that the variation of the gas density follows in the radial direction a $r^{-5/2}$ law. Which values should we take for the gas density and the mass density of the planetesimals? Since there is no reliable observational data available, we adopted in our simulations the same values as for the early solar system, namely, a nebula density ρ_g of $5.6 \simeq 10^{-9}$ g cm^{-3} at 1 AU and a mass density for the planetesimals of $\rho_{\rm pl} = 2$ g cm^{-3}. Using these values and, for instance, a radius of $s = 10$ km, the drag parameter K is $\simeq 1.3 \times 10^{-2}$. We performed simulations with different values for the planetesimal size ranging from 5 to 100 km (in diameter). This means that we varied the drag parameter K over an order of magnitude and investigated its effect on the resulting planetesimal velocity distribution. In case our adopted values for gas density and mass density are slightly wrong, our results are eventually valid for slightly different planetesimal diameters.

2.2. *Collisions*

For the collisional computations, inflated planetesimals are used in order to obtain a reasonable number of collisions per revolution. In a simulation, the dynamical evolution of typically 5000 planetesimals was followed. The planetesimals are usually distributed between 0.8 and 3.0 AU. The inflated diameter is the principal parameter that determines the optical depth of the planetesimal disk and then the collisional frequency. The choice of a suitable value of the inflated diameter or, equivalently, of impact rate is problematic since we have no clues about the possible physical parameters of the disk that might have surrounded the primary star in α Centauri. A possible strategy is to adjust the surface density of planetesimals in the α Centauri disk to that of the standard model for the solar nebula (Wetherill & Stuart 1993). Unfortunately, this does not mean that we can adopt the same optical depth as that computed for the solar nebula. The dynamics of a disk in a binary system is in fact complicated by the secular perturbations of the companion star that strongly affect the distribution of the planetesimal orbital elements. If, for example, we apply the simple relation between the mean eccentricity and inclination of a planetesimal swarm $\langle i \rangle \simeq \langle e \rangle / 2$ derived by Stewart & Wetherill (1988) for the solar nebula, we immediately see that the α Centauri disk would have a higher vertical extension compared with the solar nebula because of the larger mean eccentricity forced by the secular perturbations of the companion. The relation between $\langle e \rangle$ and $\langle i \rangle$ might, however, not hold for a disk in a binary system where the secular perturbations have a dominant role. Our simulations are bidimensional (three-dimensional simulations exceed the present CPU capabilities), and we cannot determine how the secular perturbations, once coupled to collisions and gas drag, which tends to damp the inclination as well (Adachi, Hayashi, & Nakazawa 1976), affect the average inclination of the planetesimal swarm. Unpredictable as well are the effects of the clustering in e and $\tilde{\omega}$ that, on average, increases significantly the collision rate by reducing the available phase space for the planetesimal orbit (Dell'Oro et al. 1998). In conclusion, even if the superficial density for the α Centauri disk and the solar nebula were the same, the relative optical depth may have been significantly different: the optical depth is not a suitable parameter to tune our simulations. We prefer to adopt the impact rate as the parameter that characterizes the collisional evolution of the planetesimal disk and that, therefore, determines the inflated diameter to be used in the model. We considered two different collisional frequencies as representative of the planetesimal disk in α Centauri: (1) one collision every $\sim 10^3$ yr, corresponding approximately to the impact rate of 5 km diameter planetesimals in the solar nebula; this choice requires an inflated diameter of 500,000 km; and (2) one collision every $\sim 10^4$ yr, corresponding approximately to the impact rate of 50 km diameter planetesimals in the solar nebula; this rate has been obtained by assuming an inflated diameter of 125,000 km. This same rate was used for 100 km planetesimals. It overestimates the collision rate among equal sized bodies of 100 km in diameter, but we may account in this way for the more frequent collisions of the large bodies with smaller ones, assuming that their effects are cumulative.

The collisional frequency in the simulations is computed as an average over all the radial extent of the swarm. When gas drag is included in the simulations we will see that an equilibrium state is reached, at least within 2 AU, where we are interested in showing that accretion is possible. In this case the collisional frequency is computed at the equilibrium.

The algorithm to compute the outcome of collisions consists of two major steps, namely, (1) find two planetesimals that have a mutual distance less than the critical distance for a collision (misdistance), which is equal to the inflated diameter, and (2) compute the outcome of an inelastic collision between the two bodies.

The algorithm to find close planetesimals can be very time consuming if all mutual distances between planetesimals are computed and compared with the misdistance d_m. As we will show below, the computation of all distances among the planetesimals can be avoided. We applied a so-called systolic algorithm to find nearby planetesimals: we assume n planetesimals and we assign a number to each planetesimal, numbers running from 1 to n. The planetesimals are sorted in ascending order with respect to the x-coordinates of their respective position vectors $\boldsymbol{r}$. Then, the distances between the first and adjacent planetesimals are computed and tested for a possible collision. The test on adjacent planetesimals can be terminated as soon as the difference between the x-coordinate of an adjacent planetesimal and the first planetesimal is larger than the misdistance. It is clear that only a comparatively small number of distance computations is necessary. Then, the second planetesimal is tested for possible collisions with adjacent planetesimals, and so on.

In case the distance between planetesimals i and j is less than the misdistance, an inelastic collision between the two bodies is computed in the following way. Two virtual bodies i' and j' are introduced. Body i' is situated on a line connecting bodies i and j at a distance d from body j, where d is the real, not the inflated diameter of body j. All bodies are

assumed to have the same diameter. Hence, bodies i' and j touch each other. Body i' has the same velocity as body i but corrected for the Kepler shear due to the difference between the radial distances of i and j. The outcome of an inelastic collision between bodies i' and j is computed, and a new velocity vector for body j is obtained. A corresponding computation for bodies i and j' yields the new velocity vector for body i.

For the inelastic collision computation, we follow the algorithm of Hertzsch et al. (1997). The relative velocities of two bodies are related in the normal and tangential directions after and before the collision with the help of the reconstitution coefficients ϵ_N and ϵ_T:

$$v'_N = -\epsilon_N v_N \tag{3}$$

$$v'_T = -\epsilon_T v_T \, . \tag{4}$$

We used a value of 0.3 for ϵ_N and kept $\epsilon_T = 1$ since there is up to now no sufficient experimental evidence for a dependence of ϵ_T on v_N and v_T.

2.3. *Numerical Integrator*

Two aspects determined the choice of the numerical integrator. The planetesimals can be expected to be on almost circular orbits. Otherwise, planetesimals are rapidly ejected out of the system by one of the binary stars. Hence, an integrator with a fixed step size and a low order scheme is suitable. The collision computations suggest an integrator that can easily handle instantaneous velocity changes at a given time t_c due to collisions. Therefore, numerical schemes that need data at steps preceding t_c to advance one step would not be suitable. We, therefore, decided to use a simple fourth-order Runge-Kutta integrator with fixed step size.

2.4. *Starting Values for the Planetesimals*

Numerical integrations of the equations of motion were carried out in Cartesian coordinates. The component α Centauri A is located at the origin of the coordinate system. The longitude of periastron of component B is set equal to zero. All starting values of the planetesimals were uniformly distributed and chosen at random. The starting semimajor axes range from 0.8 to 3.0 AU, and inclinations were always set equal to zero, while the remaining angle variables were chosen in the interval (0.°, 360.°). For the initial eccentricities we considered two different ranges: high values almost comparable to the forced eccentricity ($\simeq$0.05 at 1 AU) between 0. and 0.03, and low values between 0. and 0.001. We do not have any indication of the formation process of planetesimals in a binary star system and we do not know how the secular perturbations of the companion, active permanently during the evolution of the circumstellar disk, affected the initial orbital elements of the planetesimals. Low eccentricities are typical for a young planetesimal swarm in the solar system, but the perturbations of the secondary star in the α Centauri case might have influenced the formation of planetesimals forcing higher values. The two different ranges of starting eccentricities determine the distribution of the initial proper eccentricities, spread in the case [0–0.03], concentrated and almost equal to the forced eccentricity in the case [0–0.001]. In this last case we also expect an initial alignment of the periastra that are coupled to the eccentricities via the secular perturbations.

3. PERIASTRON ALIGNMENT: THE ANALYTICAL THEORY

The eccentricities and periastra of a planetesimal population revolving around the primary star of a binary system are affected by the strong secular perturbations of the companion star. Heppenheimer (1978) derived a set of equations to predict the secular evolution of the h and k variables of a test body in a binary system, with h and k defined as

$$h = e \sin(\tilde{\omega}) \tag{5}$$

$$k = e \cos(\tilde{\omega}) \, , \tag{6}$$

where e is the eccentricity of the body and $\tilde{\omega}$ its periastron longitude defined with respect to the periastron of the companion star. Introducing in the Lagrange planetary equations a development of the perturbing function, he obtained the following equations for h and k:

$$\frac{dh}{dt} = Ak - B \tag{7}$$

$$\frac{dk}{dt} = -Ah \, , \tag{8}$$

where the constants A, B are

$$A = \frac{3}{4} \frac{m_P}{n(1 - e_B^2)^{3/2}} \tag{9}$$

$$B = \frac{15}{16} \frac{ae_B}{(1 - e_B^2)^{5/2}} \, , \tag{10}$$

with e_B the eccentricity of the binary system and m_P the mass of the primary around which the test body orbits. The a and n are the semimajor axis and mean motion of the body, a planetesimal in our case, respectively. The units of mass, distance, and time are normalized in such a way that the gravitational constant G and the sum of the masses of the stars are set equal to 1, so that $G(m_P + m_s) = 1$ with m_S the mass of the companion star. The semimajor axis of the binary a_B is chosen as the unit of length, while the time is expressed in units of $(1/2\pi)T_B$, where T_B is the orbital period of the binary system.

The solution to the system of coupled differential equations can be cast in the form

$$h(t) = e_P \sin(At + \tilde{\omega}_0) \tag{11}$$

$$k(t) = e_P \cos(At + \tilde{\omega}_0) + \frac{B}{A} \, , \tag{12}$$

where e_P is the proper eccentricity. The term

$$\frac{B}{A} = \frac{5}{4} \frac{ae_B}{(1 - e_B^2)} \tag{13}$$

is the forced eccentricity e_f induced by the companion star. It is proportional to the binary eccentricity e_B. The pulsation A of the secular perturbation in e and $\tilde{\omega}$ can be read as

$$A = \frac{3}{4} \frac{\sqrt{m_P} a^{3/2}}{(1 - e_B^2)^{3/2}} \, . \tag{14}$$

Depending on the ratio between the proper and forced eccentricity, we may have libration of $\tilde{\omega}$ around 180°, or circulation. Heppenheimer gave an analytical solution for

the particular case in which the proper and forced eccentricities are equal, so that the solution always passes through the origin of the h, k coordinates.

With the secular equations in hand, we turn to the evolution of the periastra and eccentricities of a planetesimal swarm. It has been argued by Heppenheimer (1978) that, at the end of the planetesimal formation process, all the planetesimal orbits were aligned. This is a reasonable assumption if the secular perturbations of the secondary star did not influence the planetesimal formation process. In this case, the planetesimals decouple from the nebular gas and evolve under the influence of the stars' gravity with initial low eccentricities. In consequence, all the h and k values were concentrated around the origin and the periastra were aligned at the beginning of the secular evolution of the swarm. At subsequent times, the following two mechanisms contribute to spread the $\tilde{\omega}$ values.

1. The period A of the $\tilde{\omega}$ (and of the eccentricity) depends on the semimajor axis of the planetesimal. When a increases, the secular perturbation period decreases. As already noted by Heppenheimer, there is a slow dephasing process for planetesimals with different semimajor axes: the larger Δa is, the faster is the dephasing process.
2. Mutual collisions can change the values of the proper eccentricity e_P and, eventually, shift the values of $\tilde{\omega}$.

Why is the periastron alignment so important for the planetesimal accretion process? Larger impact velocities are achieved when the periastra are not aligned. At orbital crossing, the true anomalies of the colliding planetesimals are different and the radial components of the relative velocities, related to the eccentricities of the bodies, dominate over the Keplerian shear. For large eccentricities, the difference in the orbital velocity at the crossing site also contributes to increase the tangential component of the relative speed. The high impact velocities computed by Withmire et al. (1998) for the α Centauri system, and in general for other binary systems, are derived within this scenario. The companion star pumps up significant eccentricities in the planetesimal swarm with its gravitational perturbations. Since no dissipative force is included in their computations, when the periastra have lost their initial alignment and are randomly distributed, the relative velocities between planetesimals at the orbital crossing are dominated by the values of the orbital eccentricity.

However, an entirely distinct scenario is achieved when gas drag is taken into account. The combined effects of gas drag and secular perturbations of the companion star can restore a strong alignment of the planetesimals' periastra. In this condition the relative velocities are mostly determined by the Keplerian shear and may be very low in spite of high values of orbital eccentricities. The phenomenon of $\tilde{\omega}$-alignment was already observed by Marzari et al. (1997), who studied the combined effects of gas drag and gravitational perturbations by a proto-Jupiter on a swarm of planetesimals in the primordial asteroid belt. Outside of mean motion resonances, they found that the perihelia of the planetesimals were all aligned toward 270°.

An analytical justification of the alignment of periastra (or perihelia for the solar system case) can be found by introducing into the equations for the secular evolution of the variables h and k a term that models the dissipative effect of the gas drag. This works in the same way for the problem Sun-Jupiter-planetesimal as for the problem binary system–planetesimal since the equations for the variables h and k have the same structure. Since the drag would damp the eccentricities of the planetesimals at a rate proportional to e^2 (Adachi et al. 1976; Weidenschilling & Davis 1985), we can compute its effect on the variables h and k by modifying equations (7) and (8) as follows:

$$\frac{dh}{dt} = Ak - B - Dh(h^2 + k^2)^{1/2} \tag{15}$$

$$\frac{dk}{dt} = -Ah - Dk(h^2 + k^2)^{1/2} \tag{16}$$

(Greenberg 1978). According to these equations, when D is larger than A, the eccentricity is damped below B/A (the forced eccentricity) and $\tilde{\omega}$ halts its circulation and assumes a constant value that tends toward 270° for large values of the ratio D/A. Note that in these equations if the forced eccentricity is turned off ($B = 0$), the orbital eccentricity is still damped but $\tilde{\omega}$ circulates. As a consequence, if the perturber is on a circular orbit, the periastra are not aligned and the impact velocities between the planetesimals may be high, depending on the eccentricity values.

The implications of equations (15) and (16) on the collisional evolution of a planetesimal swarm are relevant. The damping term proportional to D forces planetesimals with similar semimajor axes to have the same periastra and eccentricity values (for a given a, the ratio D/A is constant). The immediate consequence is that the main contribution to the impact velocity is due to the Keplerian shear since the radial component of the relative velocity is negligible. The trajectories of the planetesimals are in fact almost parallel because of the alignment.

4. PERIASTRON ALIGNMENT: THE NUMERICAL RESULTS

4.1. *The Effects of Collisions on the Planetesimal Orbits*

In this section we analyze how collisions only, in the absence of gas drag, influence the orbital distribution of the planetesimals. Studies on the evolution of planetesimal swarms in the solar system have shown that collisions can affect the random motion of planetesimals associated with the orbital eccentricity. Stewart & Wetherill (1988) derived analytical expressions for the "viscous stirring" and "energy damping" caused by collisions, modeled as inelastic events. Depending on the characteristics of the planetesimal swarm, one of the two terms can dominate over the other. In binary systems, the scenario is complicated because of the presence of the secular perturbations of the companion star. One would expect that the impulsive changes of the orbital elements after a collision alter the proper eccentricity and the phase of $\tilde{\omega}$, destroying quickly the coherence induced by the secular perturbations. However, as we will see, the interplay between collisions and secular perturbations is more complex.

To have an insight on how collisions affect the dynamics of a planetesimal swarm, we first performed a pure N-body simulation without collisions and without gas drag: the planetesimals evolve only under the secular perturbations of the companion star. In Figures 1*a*, 1*b*, and 1*c* we show the eccentricity and periastron distributions of the planetesimals at different evolutionary times. The choice of high starting eccentricities in the range [0–0.03] generates an initial weak alignment of the periastra. All the initial h, k

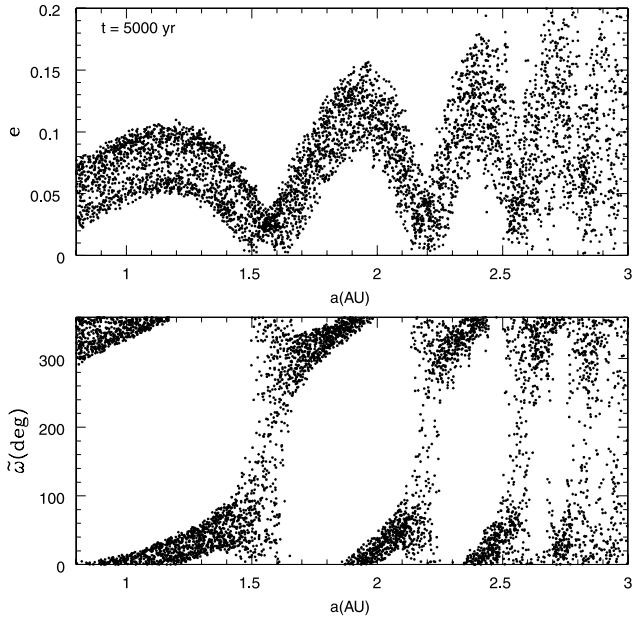

FIG. 1*a*

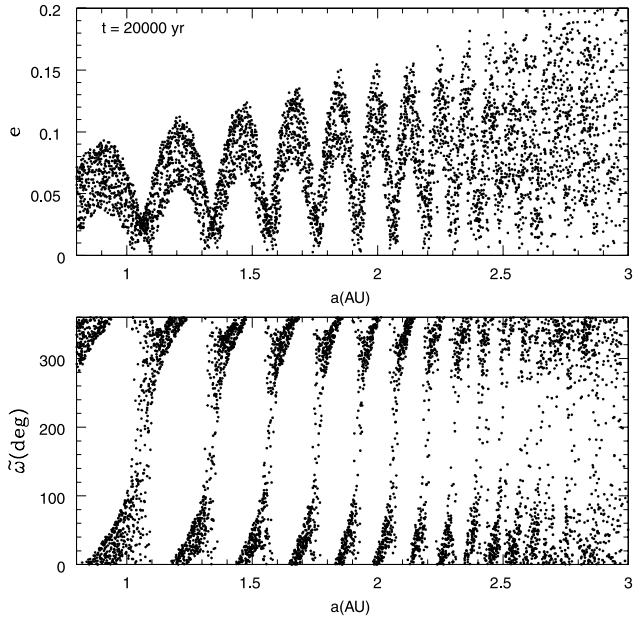

FIG. 1*b*

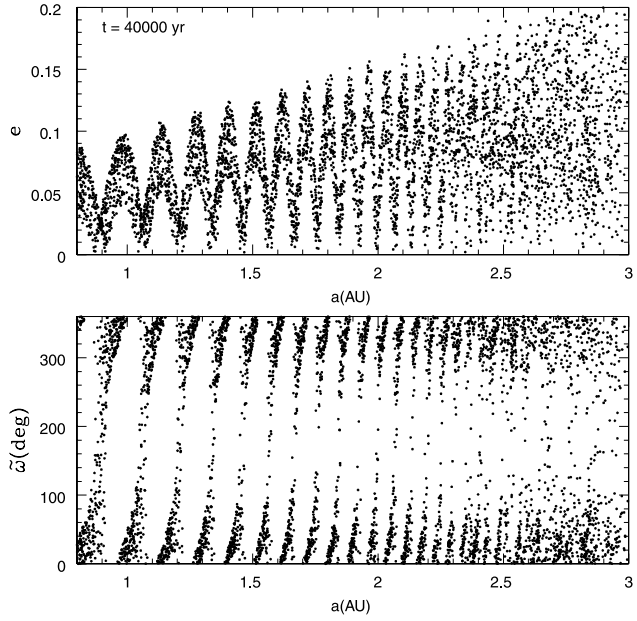

FIG. 1*c*

FIG. 1.—(*a*) Distribution of eccentricities and of periastra for the planetesimal swarm at $t = 5000$ yr. Gas drag and collisions are not included. (*b*) Same as (*a*) but for $t = 20{,}000$ yr. (*c*) Same as (*b*) but for $t = 40{,}000$ yr.

values of the planetesimals fill a circle centered at the origin (0, 0) and with radius equal to 0.03. Depending on the initial $\tilde{\omega}$, computed randomly in our simulations, different values of e_P will be assumed by each planetesimal: the maximum value of e_P will be $e_f + 0.03$. For $e_P > e_f$ the periastra circulate; otherwise they librate around 0°. The distribution in e and $\tilde{\omega}$ reflects the spreading in e_P. When the planetesimals get close to the origin (0, 0), the periastron longitudes of the circulators move fast in the h, k plane. The circulators must in fact cover a large angular span when the eccentricity approaches 0°. With increasing time, the periastra are slowly randomized, starting at larger distances from the star (Fig. 1*c*) since the period of the secular perturbations depends on $a^{3/2}$.

When collisions are included in the numerical simulations, they affect the initial distribution of e and $\tilde{\omega}$ to a different extent, depending on the semimajor axis. In Figures 2*a*, 2*b*, and 2*c* we follow the evolution in time of a swarm characterized by a high collisional frequency (1 collision every $\sim 10^3$ yr). Examining Figure 2*c*, we deduce that at small distances from the star, between 0.8 and 1.0 AU, collisions are not very effective in reducing the orbital eccentricity. The collisional damping of e works only when e itself is small, i.e., when h, k are close to the origin. In that case, the energy dissipation reduces e and, consequently, drags e_P close to e_f and $\tilde{\omega}$ close to 0° for the secular coupling. h, k are driven toward the origin (0,0). Planetesimals with similar a will have close values of e and $\tilde{\omega}$, and the

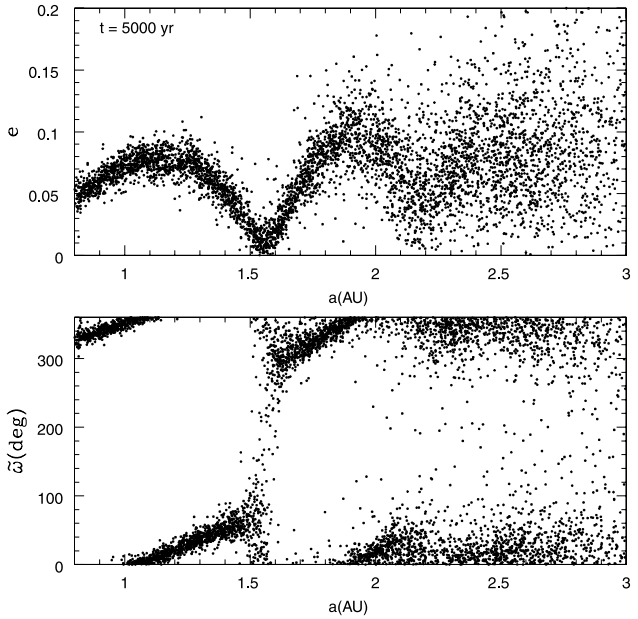

FIG. 2*a*

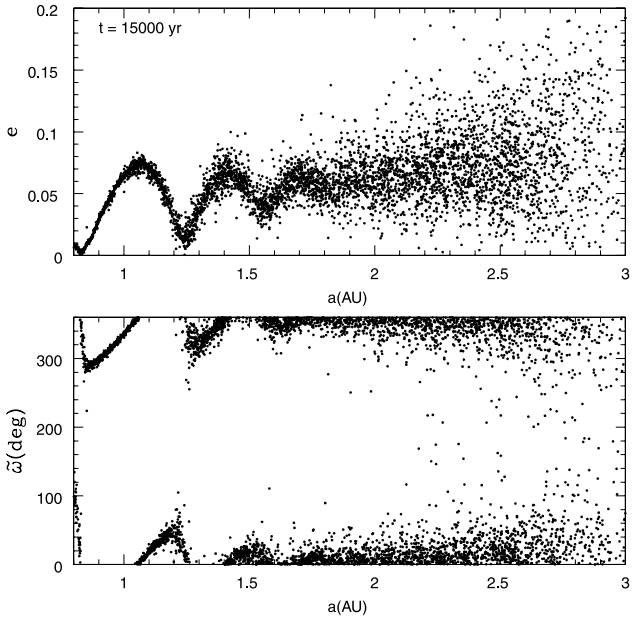

FIG. 2*b*

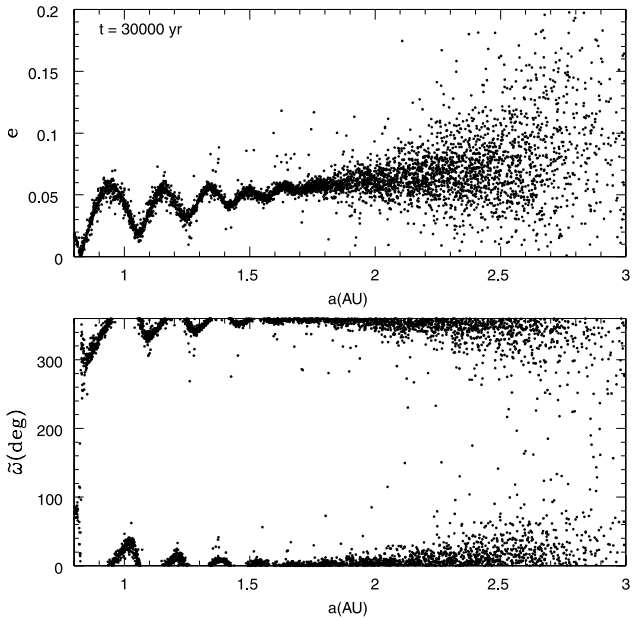

FIG. 2*c*

FIG. 2.—(*a*) Periastron and eccentricity distributions of the planetesimal swarm at $t = 5000$ yr. Collisions are included, but no gas drag. (*b*) Same as (*a*) but for $t = 15{,}000$ yr. (*c*) Same as (*b*) but for $t = 30{,}000$ yr.

initial weak alignment, due to the choice of starting values of e lower than e_f, is reinforced.

Planetesimals farther from the star, for 1.0 AU $< a <$ 2.0 AU, are very strongly perturbed by the mutual collisions that damp e significantly even when h, k are far from the origin and when the orbital e is large. Instead of driving e_P close to e_f, they tend to reduce e_P. The orbital e tends toward e_f, and the amplitude of the $\tilde{\omega}$ librations is cut down. The tendency to drive e_P close to e_f is stronger when getting farther away from the star, where collisions have a considerable damping effect. For distances larger than 2.0 AU, collisions dominate and both e and $\tilde{\omega}$ are randomized.

To test the relevance of the initial distribution of eccentricities on the evolution of the planetesimal swarm, we performed a second simulation with low starting eccentricities in the range [0–0.001]. In Figure 3 (*upper panel*) we show the final distribution of the eccentricities after 3×10^4 yr: it is almost undistinguishable from that of Figure 2*c*. Our interpretation is that the swarm loses memory of the initial distribution of the proper eccentricities on a short timescale ($\sim 10^4$ yr) to reach an equilibrium state generated by the balancing between collisional damping and secular forcing. The equilibrium distribution of the proper values of e is determined by this balancing. If we reduce the collisional frequency by a factor of 10 (Fig. 3, *lower panel*), the cumulative effects on the proper eccentricities take a longer time and cannot prevent the loss of alignment caused by the secular perturbations. On the contrary, for a semimajor axis

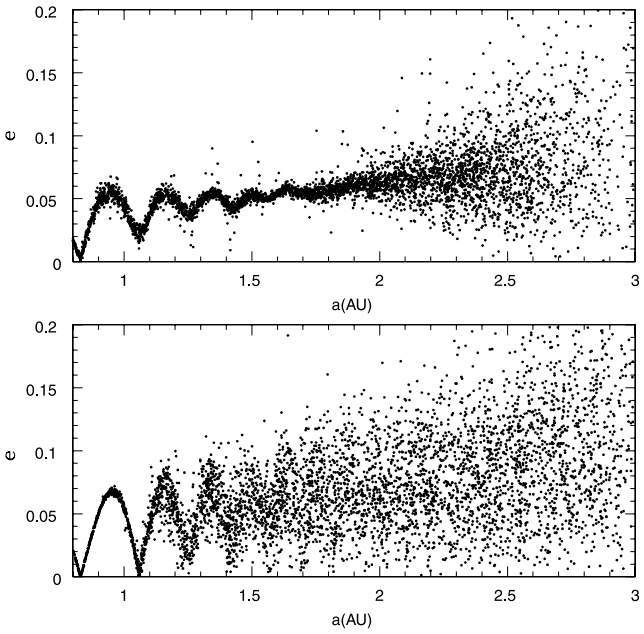

FIG. 3.—Eccentricity distributions of a planetesimal swarm at $t = 30{,}000$ yr. The upper panel illustrates the distribution of the swarm started with low initial eccentricities ($e \leq 1 \times 10^{-4}$). The lower panel shows the same distribution when a lower collision rate is adopted (1 collision every $\sim 10^4$ yr).

larger than 1.3 AU, collisions help in destroying the coherence of periastra and eccentricity, increasing then the relative velocities between the planetesimals.

4.2. *Gas Drag and Strong Periastron Alignment*

In what way does the presence of the nebular gas change the planetesimal dynamics? For small and intermediate sizes, the gas drag tends to align the periastra toward 270°, as anticipated in § 2. In Figure 4, we show the e and $\tilde{\omega}$ distribution of 5 km–sized planetesimals started on nearly circular orbits (initial e in the range [0–0.001]) after $t = 1 \times 10^4$. The alignment forced by gas drag is strong and overcomes the effects of collisions on both e and $\tilde{\omega}$ for $a < 2$ AU. Even if we increase the collisional frequency by a factor of 3 with respect to the assumed impact rate for 5 km planetesimals (1 collision every $\sim 10^3$ yr), as we did in a test simulation by altering the inflated diameter, the collisions are unable to destroy the alignment. The coherence of both e and $\tilde{\omega}$ is very strong close to the star where the density of the gas is higher. At larger distances from the primary star, the drag force diminishes since we adopt a gas density decreasing with $r^{-5/2}$. The aligned values of $\tilde{\omega}$ start from about 280° and increase up to 360° at 2 AU. Beyond 2 AU, the coherence is definitively lost: the effects of collisions and secular perturbations dominate.

For larger planetesimals, since the drag force is inversely proportional to the size of the body, we expect that the alignment is less strong. Actually, the alignment dominates the planetesimal dynamics up to diameters of 100 km. In Figures 5 and 6 we show the e and $\tilde{\omega}$ distributions for bodies of 50 and 100 km in diameter. Also in this case the initial distribution of the eccentricities is in the range [0–0.001]; the collision rate is instead low (1 collision every $\sim 10^4$ yr). With increasing diameter, the alignment is less significant and the coherence loss occurs closer to the primary star. However, in particular close to 1 AU, the values of e and $\tilde{\omega}$ of the swarm are still concentrated in a narrow range. There is a synergy between secular perturbations and gas drag that helps keep the periastra well aligned also for larger sized planetesimals. The secular perturbations by the companion contribute to the forced eccentricities of the planetesimals and are not completely damped by gas drag. According to the equations of Adachi et al. (1976), gas drag effects are stronger for larger eccentricities of the planetesimals (see also Weidenschilling, Marzari, & Hood 1998). This effect has a feedback on the $\tilde{\omega}$ alignment, which is reinforced. We can say that the secular perturbations of the companion star help keep the impact velocities low by increasing the eccentricities and, thus,

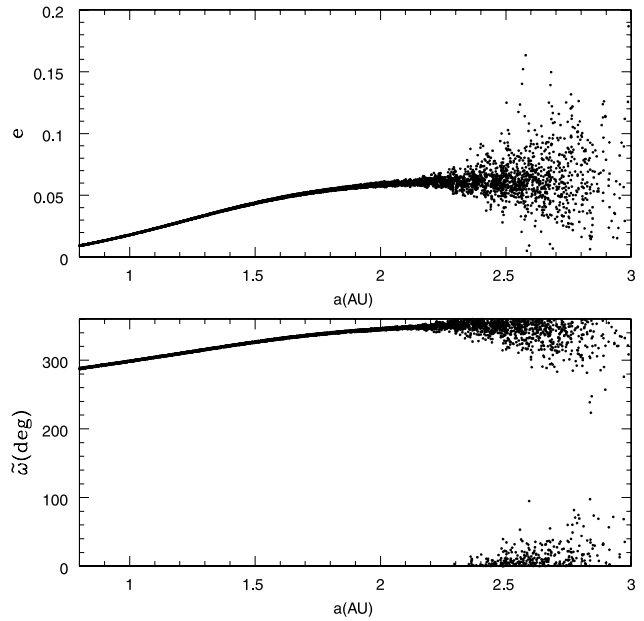

FIG. 4.—Periastron and eccentricity distributions of a swarm of 5 km diameter planetesimals at $t = 1 \times 10^4$. Collisions and gas drag are included.

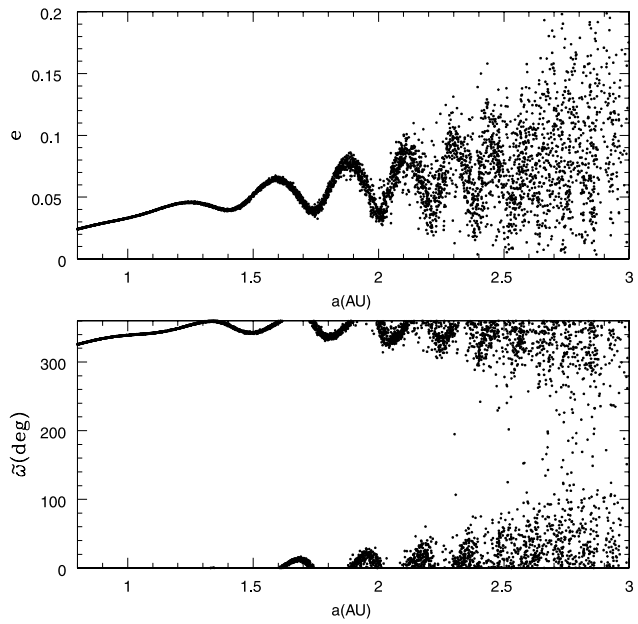

FIG. 5.—Same as Fig. 4 but for 50 km–sized planetesimals

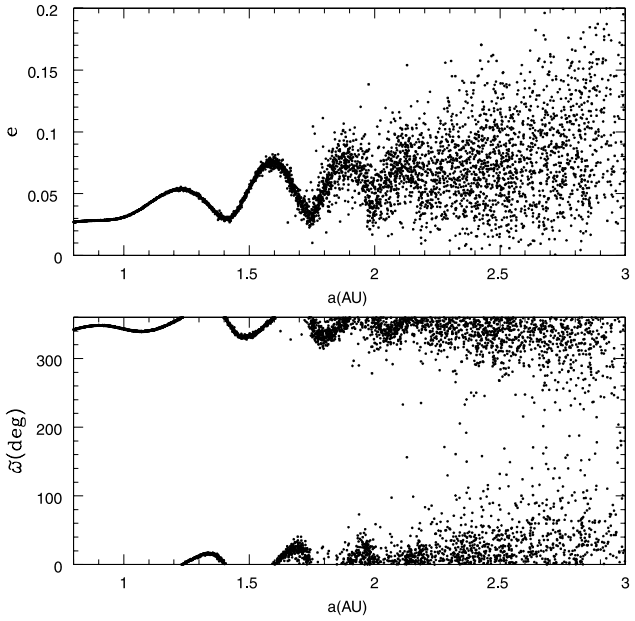

FIG. 6.—Same as Fig. 4 but for 100 km diameter planetesimals

favoring the gas drag to align the periastra. For the relative impact velocities of planetesimals, this phenomenon is of particular importance.

4.3. *Distribution of the Impact Velocities*

In a planetesimal swarm where the eccentricities are all concentrated in a narrow range and where the periastra are all aligned, the relative velocities at planetesimal encounters are mostly determined by the Keplerian shear. This effect is illustrated in Figure 7, which shows the impact velocities versus time for 5 km–sized planetesimals in the range between 0.8 and 1.2 AU from the primary star. At $t = 0$, the orbital elements are randomly distributed and the impact velocities are of the order of 1–1.5 km s^{-1}. As the periastra and eccentricities align because of the effects of gas drag and secular perturbations, the impact velocities progressively decrease to values of the order of a few m s^{-1}. An equilibrium state is reached with all the periastra aligned, and the impact velocities remain low during the subsequent evolution of the swarm.

In a planetesimal population characterized by different sizes of the bodies and covering a large range in semimajor axis, the balance between gas drag, collisions, and secular perturbations can change significantly. The degree of periastron alignment depends on both the diameter D and distance R from the star. We compare in Figures 8*a*, 8*b*, and 8*c* the distributions of encounter velocities for different values of D (5, 50, and 100 km) and for R ranging from 0.8 to 2.4 AU. The sizes of the bodies are computed adopting a bulk density ρ equal to 2 g cm^{-2}. The velocities are taken after the equilibrium state is reached (10^4 yr), and the distribution is computed over a time interval of 2000 yr. In each panel of Figure 8, we also draw as reference the velocity v_{fr} for which bodies begin to fragment rather than accrete. v_{fr} is calculated with the semiempirical model described in Davis et al. (1989), Spaute et al. (1991), Petit & Farinella (1993), and Marzari, Davis, & Vanzani (1995). The fraction f_{KE} of the collisional energy partitioned into the fragments was assumed to be 0.05. We define as v_{fr} the velocity for which 50% of the mass of each of the two bodies escapes.

For planetesimals 5 km in diameter (Fig. 8*a*), accretion dominates for radial distances less than 2.4 AU. This is confirmed in Table 1, where we report the median of the distribution for each interval of distance and we compare it

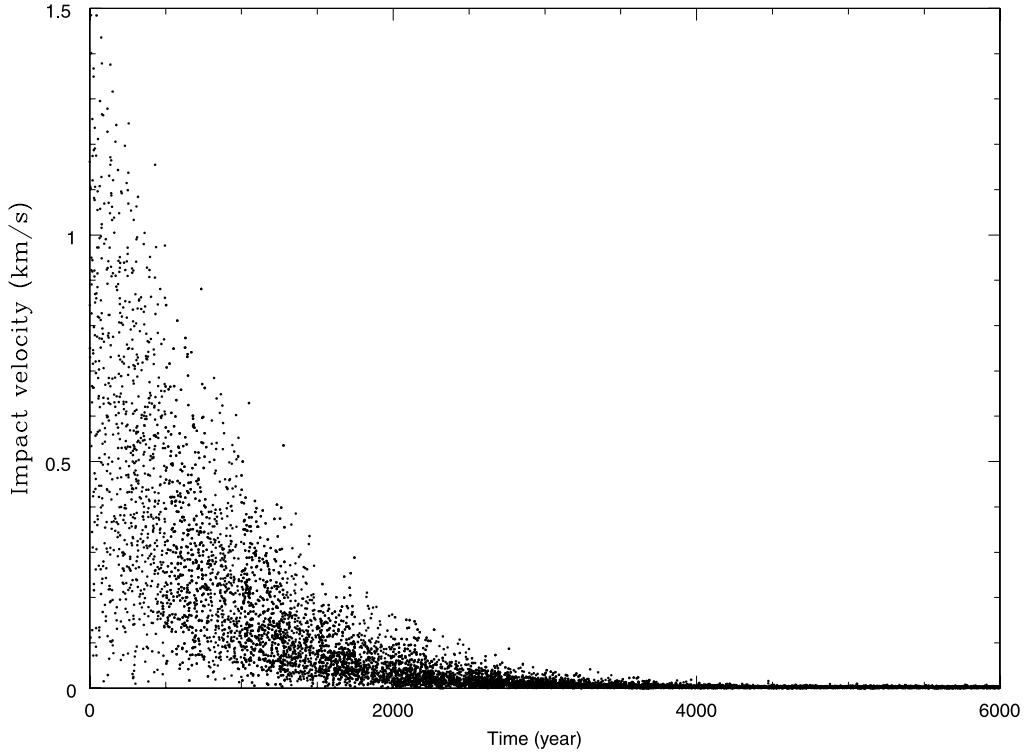

FIG. 7.—Evolution of the impact velocities with time in the swarm of 5 km planetesimals

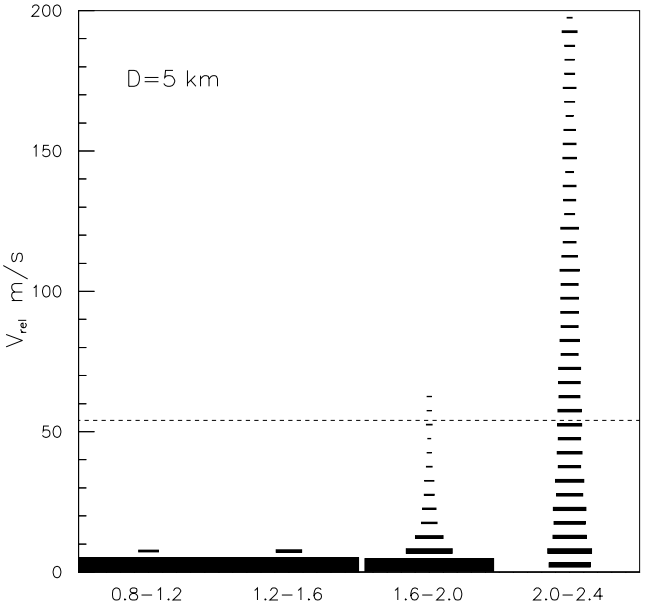

FIG. 8*a*

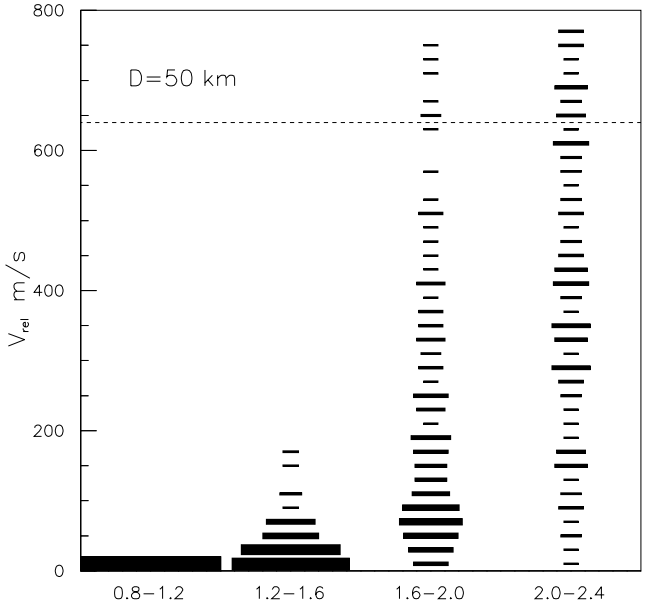

FIG. 8*b*

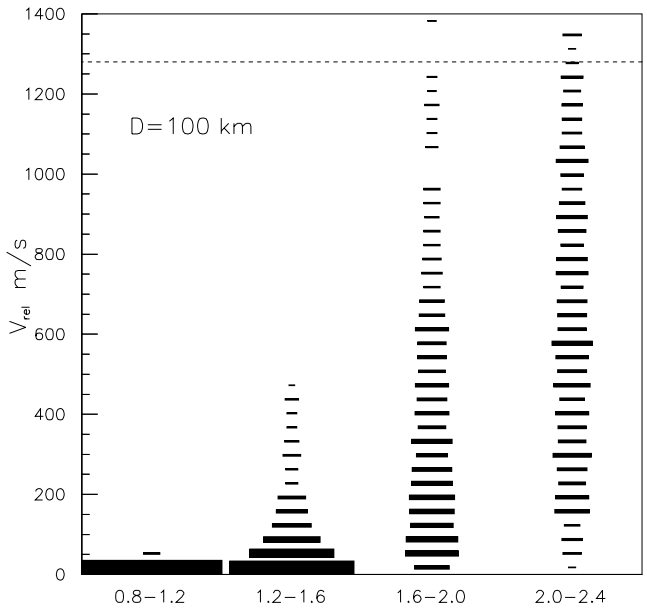

FIG. 8*c*

FIG. 8.—(*a*) Distribution of the relative velocities between 5 km–sized planetesimals at different distances from the primary star. The dashed line represents the maximum speed before fragmentation dominates. (*b*) Same as (*a*) but for 50 km–sized planetesimals. (*c*) Same as (*b*) but for 100 km–sized planetesimals. (See the electronic edition of the Journal for a color version of this figure.)

with v_{fr}. For larger planetesimals, the distributions extend to higher relative velocities since the gas drag is less efficient. However, as confirmed in Figures 8*b* and 8*c* and in Table 1, accretion dominates also for bodies of 50 and 100 km diameter. To illustrate the effectiveness of periastron and eccentricity alignment in reducing the encounter velocities, in Figure 9 we show the relative velocities for a swarm of planetesimals where the dynamical effects of gas drag are switched off by setting the gas density equal to 0. Even higher impact speeds are obtained when also the effects of the collisions are cancelled by fixing the restitution coefficient at each encounter to 1 (Fig. 10). In this last pure three-body model, which reproduces closely the one adopted by Whitmire et al. (1998), the relative velocities would not allow accretion for bodies smaller than 100–200 km in diameter. In the last three lines of Table 1 we give the medians of the relative velocity distributions for the case [no-gas] with high and low collisional frequency and for the case [no-gas, no-collisions] (pure three-body case).

According to the results summarized in Table 1, accretion of planetesimals into larger bodies and planets is possible in the terrestrial region of the α Centauri system within the critical semimajor axis of Holman & Wiegert (1999). At the beginning of the planetesimal accretion, when the bodies are small, the gas drag gives a fundamental contribution by aligning the periastra and lowering the impact velocities. This allows accretion to continue in spite of the strong secular perturbations of the companion star. When larger

TABLE 1

MEDIANS OF THE RELATIVE VELOCITY DISTRIBUTIONS BETWEEN PLANETESIMALS OF DIFFERENT SIZES AT DIFFERENT DISTANCES FROM THE PRIMARY STAR

	r-Zone				
Size (km)	[0.8–1.2] (m s^{-1})	[1.2–1.6] (m s^{-1})	[1.6–2.0] (m s^{-1})	[2.0–2.4] (m s^{-1})	Fragmentation (m s^{-1})
5	1.7	1.9	2.1	51.2	54.
50	1.3	21.9	124.0	521.6	640.
100	3.6	34.1	270.0	621.6	1280.
No Gas (HCF)	137.2	323.2	519.3	713.4	...
No Gas (LCF)	154.4	722.1	970.3	1295.4	...
No Gas–No Collision	818.3	855.7	1092.1	1233.1	...

NOTES.—The corresponding velocities for which fragmentation occurs are given in the last column. In the two lines of the table titled "No Gas" the relative velocities are computed when collisions are included but no gas drag, for high collisional frequency (HCF; Fig. 2*c*) and low collisional frequency (LCF; Fig. 3, *bottom panel*). In the last line of the table the impact speeds are computed in a pure three-body problem in the absence of gas drag and collisions.

sizes are obtained ($\geq$150 km) the gas drag is less efficient in producing the periastron alignment. However, relative velocities are lower than v_{fr}, which is about 1.5 km s^{-1} for bodies of 150 km in diameter. Thus, accretion can continue to form larger objects.

5. DISCUSSION

Relative velocities between planetesimals determine whether or not accretion is possible. If they are too high, fragmentation dominates and planetesimals do not grow but comminute. Critical in this sense are the initial phases of the accumulation process, when all the planetesimals have approximately small sizes ($\leq$10 km in diameter). During an impact between two small bodies, the gravity may not be strong enough to prevent the collisional fragments from escaping. Planetesimal encounter velocities of some tens of meters may in effect cause dispersion of the fragments rather than accretion.

In close binary systems, encounter velocities in a swarm of planetesimals surrounding one of the stars may be excited to high values by the gravitational perturbations of the companion. In a system like α Centauri, which is a typical close binary system, the forced eccentricity due to the companion secular perturbations are of the order of ~0.05 in the terrestrial zone (0.8–3 AU). If the orbital angles of the swarm are randomized, the resulting eccentricities lead to impact velocities of the order of 1–1.5 km s^{-1}, enough to prevent accretion of planetesimals smaller than 150 km in diameter. If the initial planetesimal disk was formed by small bodies ($\leq$10 km), the formation of planets might have been inhibited.

The scenario totally changes if we consider the effects of the gas drag. The gas drag force coupled to the secular perturbations due to the companion star causes a strong periastron alignment that drastically diminishes the encounter velocities of planetesimals in spite of large eccentricities. We investigated the relative velocity distributions in the α Centauri system including in our numerical model both the effects of gas drag and collisions. The alignment of periastra significantly reduces the radial component of

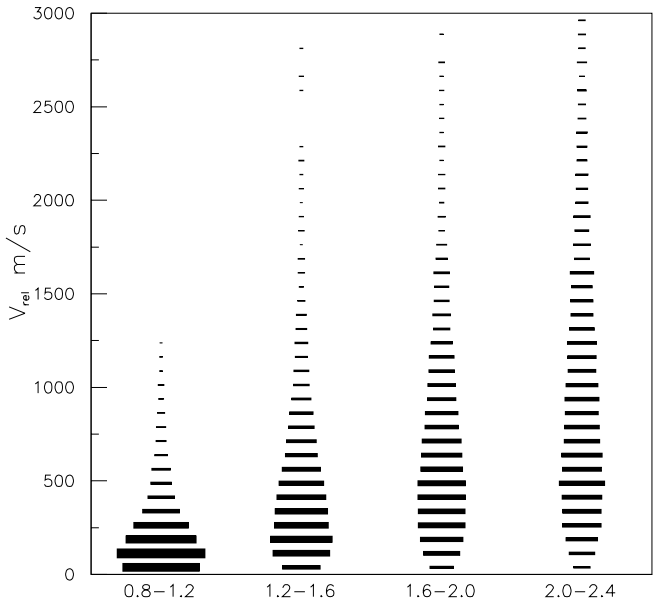

FIG. 9.—Velocity distribution of planetesimals at different distances from the primary star. Gas drag effects are not included in the simulation. (See the electronic edition of the Journal for a color version of this figure.)

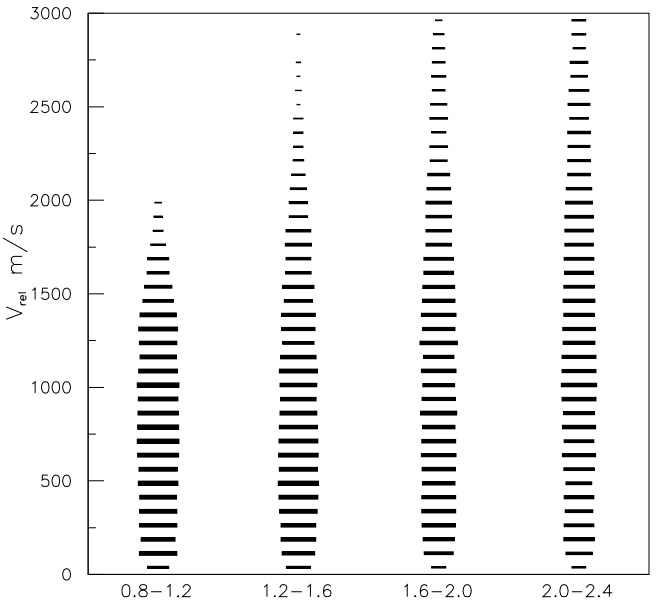

FIG. 10.—Same as Fig. 9 but gas drag and the effects of collisions are not included. (See the electronic edition of the Journal for a color version of this figure.)

encounter velocities. Keplerian shear dominates. Impact velocities are significantly lower than the critical velocity for fragmentation: accretion may occur at all planetesimal sizes.

Although accurate, our numerical modeling is based on some simplifications required by the difficulty of including in a single algorithm collisions and dynamical evolution. The amount of CPU time needed to complete a single run of the code has also forced us to introduce some approximations in the simulations. Our results are obtained assuming an initial two-dimensional distribution of the planetesimals to keep the CPU time for a single simulation within 1 month on a fast computer. However, the two-dimensional results can be extended to three dimensions, at least until the perpendicular component of the encounter velocity, due to the inclination of the orbits, does not overcome the Keplerian shear. The periastron alignment, as we confirmed in some test numerical integrations without collisions, persists at high inclinations (up to 30°). The amount of CPU time also constrains the number of bodies that can be included in a simulation.

In our algorithm, collisions are assumed to be inelastic. This modeling is incomplete since it does not include all the possible outcomes of a collisional event. However, even if it cannot describe the evolution of the planetesimal size distribution, it approximates quite well the dynamical effects of collisions on the planetesimal swarm, in particular what concerns the orbital element distribution. A similar algorithm has already been used by Thebault & Brahic (1999) to analyze the effects of collisions in the early asteroid belt in mean motion resonances with Jupiter. Moreover, in our simulation the periastron alignment due to gas drag is so strong that our results are robust in spite of the incompleteness of the collisional model. The combined effects of gas drag and secular perturbations dominate over collisions. For the same reason we expect that, in addition, the mutual gravitational perturbations between planetesimals, which are not included in our model, do not significantly affect our results. The situation might change and the mutual perturbations might be influent when large embryos form within the planetesimal swarm. It would also be interesting to investigate whether the formation of the embryos occurs via runaway growth or orderly growth. This is under investigation and will be described in a forthcoming paper.

We thank P. Thebault for useful comments and suggestions.

REFERENCES

Adachi, I., Hayashi, C., & Nakazawa, K. 1976, Prog. Theor. Phys., 56, 1756
Akeson, R. L., Koerner, D. W., & Jensen, E. L. N. 1998, ApJ, 505, 358
Davis, D. R., Weidenschilling, S. J., Farinella, P., Paolicchi, P., & Binzel, R. P. 1989, in Asteroids II, ed. R. P. Binzel, T. Gehrels, & M. S. Mattews (Tucson: Univ. Arizona Press), 805
Dell'Oro, A., Marzari, F., Paolicchi, P., Dotto, E., & Vanzani, V. 1998, A&A, 339, 272
Dominik, C., Laureijs, R. J., Jourdain de Muizon, M., & Habing, H. J. 1998, A&A, 329, L53
Greenberg, R. 1978, Icarus, 33, 62
Heppenheimer, T. A. 1978, A&A, 65, 421
Hertzsch, J.-M., Scholl, H., Spahn, F., & Katzorke, I. 1997, A&A, 320, 319
Holman, M. J., & Wiegert, P. A. 1999, AJ, 117, 621
Kary, D. M., Lissauer, J. J., & Greenzweig, Y. 1993, Icarus, 106, 288
Marzari, F., Davis, D. R., & Vanzani, V. 1995, Icarus, 113, 168
Marzari, F., Scholl, H., Tomasella, L., & Vanzani, V. 1997, Planet. Space Sci., 45, 337
Mathieu, R. D. 1994, ARA&A, 32, 465
Mathieu, R. D., Ghez, A. M., Jensen, E. L. N., & Simon, M. 2000, in Protostars and Planets IV, ed. V. Mannings, A. Boss, & S. S. Russell (San Diego: Academic)
McCaughrean, M. J., & O'dell, C. R. 1996, AJ, 111, 1977
Petit, J.-M., & Farinella, P. 1993, Celest. Mech. Dyn. Astron., 57, 1
Rodriguez, L. F., et al. 1998, Nature, 395, 355
Spaute, D., Weidenschilling, S. J., Davis, D. R., & Marzari, F. 1991, Icarus, 92, 147
Stewart, G. R., & Wetherill, G. W. 1988, Icarus, 74, 542
Thebault, P., & Brahic, A. 1999, Planet. Space Sci., 47, 233
Trilling, D. E., & Brown, R. H. 1998, Nature, 395, 775
Trilling, D., Brown, R., & Rivkin, A. 2000, ApJ, 529, 499
Weidenschilling, S. J., & Davis, D. R. 1985, Icarus, 62, 16
Weidenschilling, S. J., Marzari, F., & Hood, L. L. 1998, Science, 279, 681
Wetherill, G. W., & Stewart, G. R. 1993, Icarus, 106, 190
Whitmire, D. P., Matese, J. L., Criswell, L., & Mikkola, S. 1998, Icarus, 132, 196